



PERFORMANCES EVALUATION AND BLADE NUMBER OPTIMIZATION OF RADIAL INFLOW TURBINE

**Sid Ali LITIM^{1*}, Habib BENZAAMA¹, Mohammed HAMEL²,
Mohamed Kamel HAMIDOU², Abidine DEBAB²**

¹Department of Mechanical Engineering, National Polytechnic School of Oran Maurice Audin (ENPO-MA), El Mnaouar BP 1525 Es Senia road, Algeria

²Department of Mechanical Engineering, Faculty of Mechanical Engineering, University of Sciences and Technologies Mohamed Boudiaf of Oran, El Mnaouar, BP 1505, Bir El Djir, Algeria

ABSTRACT

The energy exhaust recovery in engines is obtained using turbochargers which are widely used in the automotive industry. A turbocharged engine leads to a better overall system efficiency and a reduction in exhaust emissions compared, at constant power, with a naturally aspirated engine. The numerical approach in the present work is to explore ways of improving the performances of the radial inflow turbine. This work investigates the performances of a radial inflow turbine under steady states conditions and how they are affected by the rotor geometry. The radial inflow turbine is investigated numerically using 3D Reynolds averaged Navier-Stokes equations, the objective here is to determine the optimum of performance characteristics of the turbine. The building of the geometry and the generation of unstructured meshes are achieved using ANSYS-ICEM software whereas in order to simulate the flow, the ANSYS-CFX code is applied. The numerical method is also used to determine optimum geometrical characteristics such as the optimum of blade number. It has been found that the rotor with 12 blades gives better performances.

Key words: Radial inflow turbine, Performance, Efficiency, Finite volume method, Ansys-CFX.

Cite this Article: Sid Ali LITIM, Habib BENZAAMA, Mohammed HAMEL, Performances Evaluation and Blade Number Optimization of Radial Inflow Turbine, *International Journal of Advanced Research in Engineering and Technology (IJARET)*, 12(11), 2021, pp. 85-97.

<https://iaeme.com/Home/issue/IJARET?Volume=12&Issue=11>

1. INTRODUCTION

Modern diesel engines are equipped with turbochargers to improve fuel economy, enhance engine power, and reduce pollutant emissions. They were used mainly in the field of marine propulsion when they first appeared and in recent years have become widely used for road transport. Presently the radial inflow turbines are widely spread in automotive applications and auxiliary power units using turbocharger technology. Radial turbines are characterized by compact design, higher efficiency at high revolutions, low expansion ratios, and high power-to-weight ratios. They retain a high efficiency when smaller, and can operate at high expansion ratios on one single stage. As for axial turbines which are generally used for large turbocharger engines in marine and railway applications for instance, they are constituted by several stages. The components of a radial turbine are classified as follows: the inlet volute, the stator nozzle, the rotor and finally the exhaust diffuser as shown in figure 1.

The design of the rotor is investigated because it is the element that influences most the performance of the entire turbine. Blade channel geometry influences the elaborated mass flow rate. Flow motion from the end of the blade towards the hub radius determines power production and thus work exchange. It also reduces the speed of tangential component that accounts for work exchange. Also, the tangential component of the flow is reduced, resulting in a high pressure gradient along the blade to blade channel. At the output of the rotor, the flow is axial, the radial velocity component is zero, and the flow angle is 90° . Rodgers and Geiser [1] correlated attainable efficiency levels of radial inflow turbine versus the blade tip speed/spouting velocity ratio (loading coefficient) ie U_2/c_0 and the axial exit flow coefficient ie c_{m3}/U_2 . These results are illustrated in Fig. 2. From this figure it can be seen that peak efficiency values are obtained with velocity ratios close to 0.7 and with values of exit flow coefficient between 0.2 and 0.3 (Dixon 1998) [1].

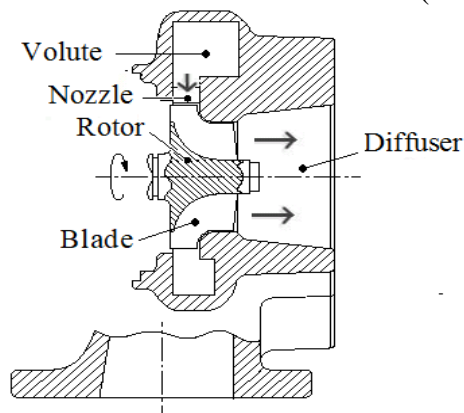


Figure 1 Cross section of the radial inflow turbine

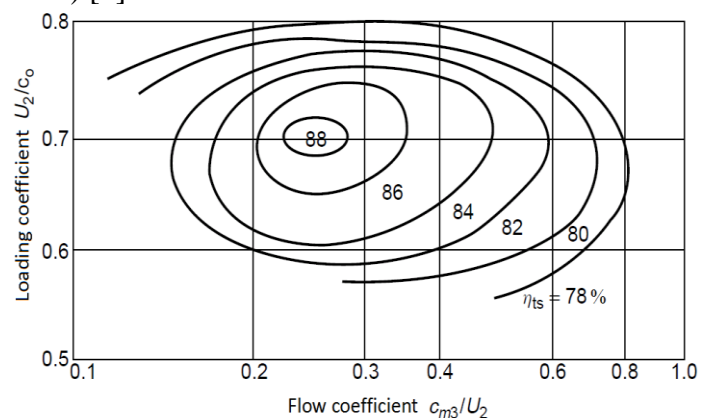


Figure 2 Loading and Flow Coefficients [1]

Radial turbines have been extensively investigated, both experimentally and numerically, at NASA Lewis Research Centre, starting in the mid1960s. Rohlik [3] has performed the analysis on the performance of the radial turbine in order to obtain the optimum geometry. These introductory notes will be illustrated primarily on one-dimensional computational models that have been developed in the past. Todd et al. [4] describe a computational code using the model reported by Futral et al. [5] to predict the out-of-design performance of a radial flow turbine. An improved version of the computational code described in [4] is presented by Wasserbauer et al. [6], which presents better loss models than those implemented in [5], to take into account the trailing edge blocking, and calculate the flow conditions for equal or higher pressure ratios beyond the stator and/or rotor setting [7]. Several studies have been carried out using commercial computational codes to improve the performance of radial-aspirated turbocharger turbines.

To improve the aerodynamic efficiency of radial and mixed inflow turbocharger turbine having 12 blades, Khairuddin et al. [8] describe an optimization procedure to modify their geometry. The procedure integrates parameterization of the turbine blade geometry and the genetic algorithm optimization. The analysis of 3D CFD is obtained using a commercial solver. The hub and shroud profiles were observed to have the important impact on turbine performance, optimization of which leads to an increase of 1.3 percentage points of efficiency.

However, Zhang et al. [9] state that the hub and shroud slope will have the most influence on the performance of the turbine at the initial design stage. In general, no method is available to calculate the optimal number of blades for a given task. The methods available to calculate the number of blades are empirical and they lead to different numbers of blades for the same geometry [2]. A large number of vanes is necessary for better guidance of the flow and to avoid flow reversals of increased friction losses and flow blockages. Eventually, a reasonable compromise solution can be found.

The radial inflow turbine shown in Figures 3 and 4 was developed by Kerry et al. [10] to drive a compressor stage with a mass flow rate of 0.414 kg/s and a rotational speed of 70000 rpm. The turbine inlet temperature at the design point is 923 K. The experimental tests by Kerry et al. and Chen et al. [11] were conducted in air at nominal turbine inlet conditions of 333.82 K. Under these conditions, with the engine hot, the Reynolds number was obtained at design values corrected for mass flow, and speed.

The data were obtained at speeds from 0 to 100 percent of the corrected design speed at corrected ratios of the turbine inlet total static pressure to the rotor outlet static pressure of 1.2 to 2, 97. Overall performance is presented in terms of reduced mass flow, pressure ratio, speed ratio, and efficiency. The turbine design operating conditions are given in Table 1.

Table 1 Design conditions of the radial inflow turbine

Rotational speed	70000 rpm
Mass flow rate	0.414 kg/s
Inlet total temperature	923 K
Pressure ratio	1.21 ~ 2.97
Optimum velocity ratio	0.64

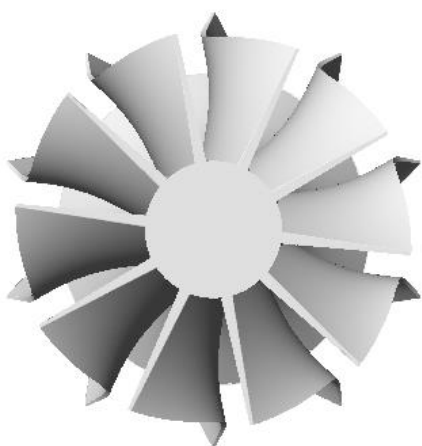


Figure 3 Radial inflow rotor

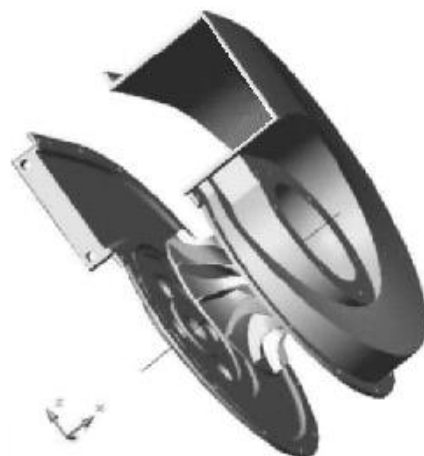


Figure 4 Radial inflow turbine of turbocharger

This study presents a numerical predictions of radial inflow turbine performance for a wide pressure ratios range. It also investigates the influence of the number of blades on the performance on the radial inflow turbine. The computational tests are carried out with the

ANSYS-CFX software on a passage from blade to blade (figure 3) using the k- ϵ turbulence model. First the computed results are compared with the experimental data, secondly study of the number of blades on the radial inflow turbine performances is made. The overall geometric characteristics of the turbine are presented in Table 2.

Table 2 Turbine geometrical characteristics

Rotor inlet diameter	150.4 mm
Ratio of rotor exit tip to inlet diameters	0.6275
Ratio of rotor exit hub to tip diameters	0.4844
Ratio of stator exit to rotor inlet diameters	1.111
Ratio of stator inlet vane height to rotor inlet diameter	0.0726
Ratio of stator exit bane height to rotor inlet diameter	0.0537
Rotor exit mean blade angle	-24 deg
Rotor axial length	40.00 mm
Number of blades	10

2. MESH GENERATION

The highly three-dimensional, compressible, viscous, and turbulent flow in the radial inflow turbine shown in Figures 4 and 5 is obtained by numerically solving the averaged Reynolds equations of mass, momentum, and energy conservation. Temperature, pressure, and density are related by the equation of state. Turbulence is modelled by the standard k- ϵ equation of Patankar and Spalding [12]. This model is based on the concept of turbulent viscosity which assumes that Reynolds stresses can be expressed in terms of mean velocity gradients and turbulent viscosity in a manner analogous to viscous stresses for Newtonian laminar flows.

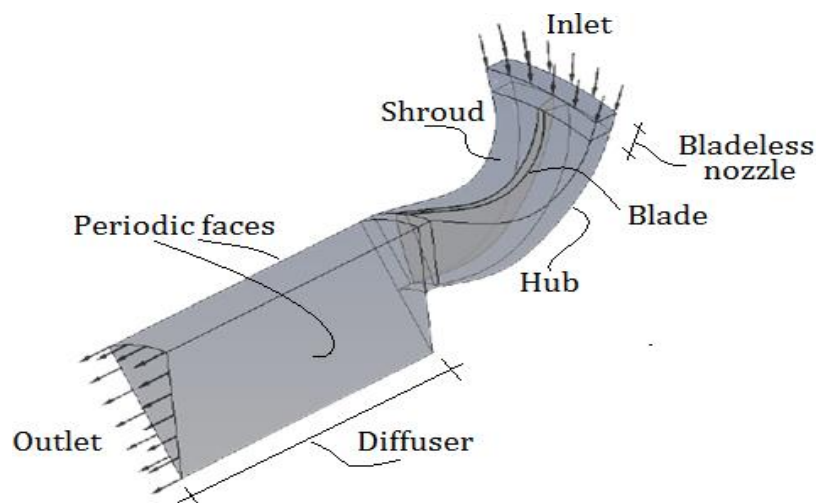


Figure 5 Radial inflow rotor channel

2.1. Numerical Method

The flow solution in the radial inflow turbine, shown in figure 6 and 7, is obtained by the finite volume approach. The geometry of the vane channel is constructed using the ANSYS ICEM CFD software, then the entire domain is discretized by an unstructured mesh of hexahedral elements as shown in figure 5.

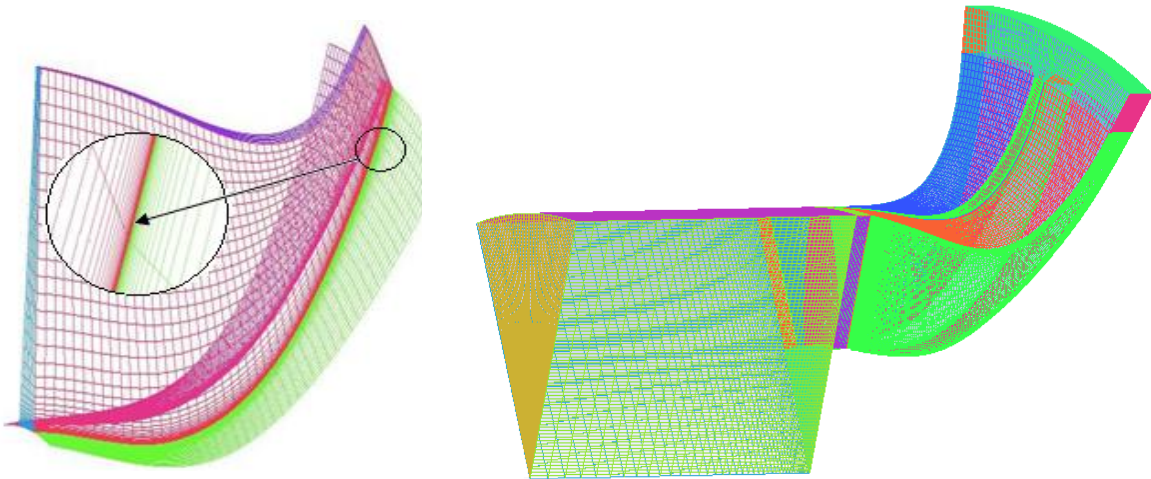


Figure 6 Blade mesh refinement

Figure 7 Unstructured mesh of the blade-to-blade channel

The influence of the pressure ratios on the turbine performance is done on a one blade to blade channel with periodic conditions on the middle meridian surface. A blade passage including the exhaust pipe is illustrated in figure 5.

During the mesh generation process, caution must be taken in choosing the first grid spacing near the boundaries of the walls to achieve the correct resolution of the boundary layer. Due to the use of the wall function approach to model the flow near the wall in the $k-\epsilon$ turbulence model, it is advisable to include the y^+ value for the node near the wall between 20 and 100 [13].

2.2. Resolution Method

The integration on finite volumes of the equations describing the turbulent flow leads to a set of discrete equations. The terms of the differential equations on the volume interfaces are obtained by a second order upwind scheme.

As opposed to the unstaggered grid which uses four mesh in order to determine the flow parameters i.e. the three velocities (u , v , w) and the pressure P , CFX-ANSYS uses an algorithm called (Coupled solver) where only a single cell is used for the calculation of these parameters. The method is similar to that used by Rhie and Chow [14] to prevent the disturbance of the pressure field because of the unstaggered grid. This method is among the methods that best save memory space and the computation time performed by the solver. The flow is assumed to be subsonic at the domain inlet and thus the total pressure and the total temperature in the stationary frame of reference as well as the flow direction and the intensity of turbulence ($I=5\%$) are imposed. At the outlet where a subsonic flow is assumed, the static pressure is imposed. A no slip condition is applied on the solid boundaries. Because of the use of only one blade passage, a periodic boundary condition is assumed at the left and the right of the computational domain. The conditions of the numerical tests are given in table 3.

Table 3 Numerical conditions

Rotational Speed (rpm)	Total Inlet Temperature (K)	Pressure Ratio Range
31456 (50%)	333.82	1.218 ~ 1.545

3. RESULTS AND DISCUSSIONS

3.1. Overall Comments

First, the numerical method described in this work was used to compare the results obtained numerically and experimentally, different performance tests are used for the rotor inlet flow conditions on the 10-blade radial turbine [10] and [11]. Second, the model is used to study the effect of the number of blades on the turbine performance without taking into account the volute effect on the machine as all together. As indicated by Pullen [15], the tests showed that the presence and the rotor speed had a negligible influence on the volute flow field. The volute accelerates and guides the flow of fluid to the rotor with an optimum entry angle, uniformity of thermodynamic parameters, speed, and Mach number. The volute performance is dependent on the geometric shape of the single or double entry cross-section, the length, and the tab shape. Such a volute could correspond to the considered rotor.

3.2. Grid Solution

Four mesh sizes as shown in Table 4 were used to obtain the solution for the turbulent flow in order to choose an optimal grid for the final calculation. The solutions obtained with the four grids are presented in figure 6 and 7, represents the influence of the grid size on a solution in terms of pressure distribution at mid-distance from the blade. Grid (D) with 385459 elements was found to give a satisfactory solution and was used for the calculation of the test cases.

Table 4 Numerical Mesh size for grid dependency of the solution

Mesh size			
(A)	(B)	(C)	(D)
145723	245595	321096	385459

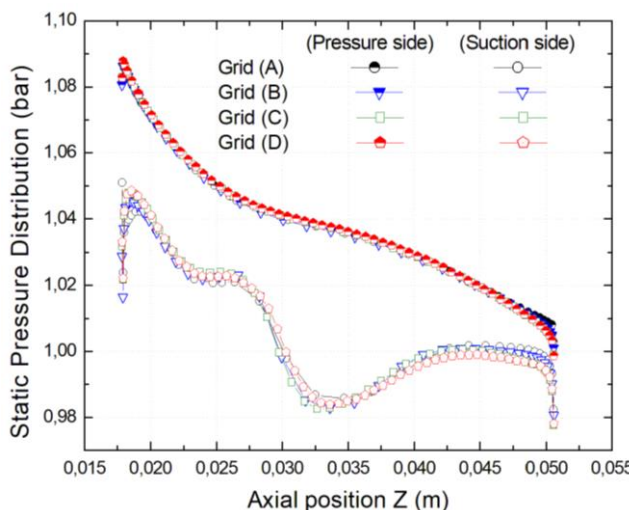


Figure 8 Effect of the number of elements on the solution (50 % Speed, $Pr = 1.218$, $T_0^* = 333.82$ K)

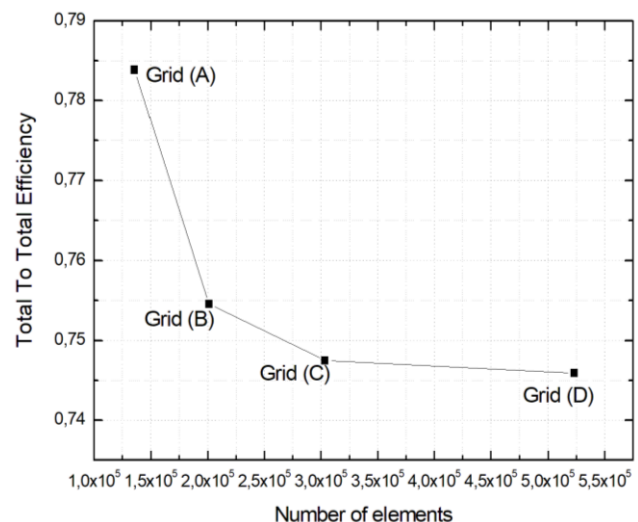


Figure 9 Effect of the number of elements on efficiency

In order to quantitatively estimate the discretization error, the GCI (Grid Convergence Index) is calculated on the basis of Celik et al. [16] using the calculated mass flow as a significant variable. The maximum value of the GCI is 0.15% indicating that the discretization error has very little influence on the convergence towards the asymptotic solution. To validate the numerical model, the numerical tests of the 10 blade radial turbine were compared with the experimental data of Chen et al. [11] for a pressure ratio of 2.5 bar and a rotation speed of 70 000 rpm. Figure 10 shows the variation of the static pressure at the same time as the ferrule, one notes a good agreement of the numerical and experimental results.

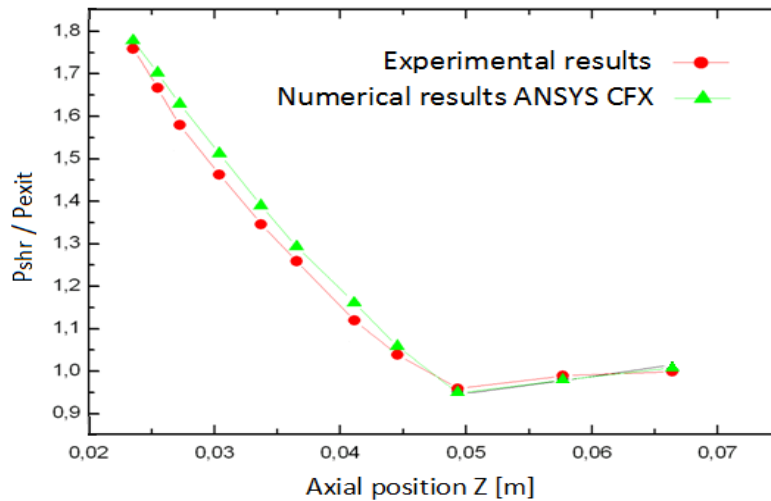


Figure 10 Variation of the pressure ratio (Pshr/Pexit) along the shroud Pr = 2.5 and 100 % speed)

3.3. Performance Characteristics

Figures 11 to 14 show the comparison of performance characteristic tests obtained experimentally and numerically of the radial inflow turbine. We observe that all the curves have a similar shape and present a satisfactory agreement between the computed and the measured result. Figure 11 show the computed mass flow rate characteristics in terms of pressure ratio versus the reduced mass flow rate defined as:

$$Pr = P_{0^*}/P_{exit} \quad (1)$$

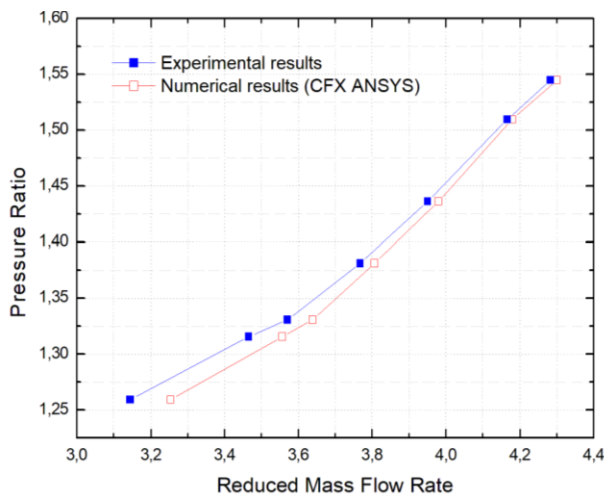
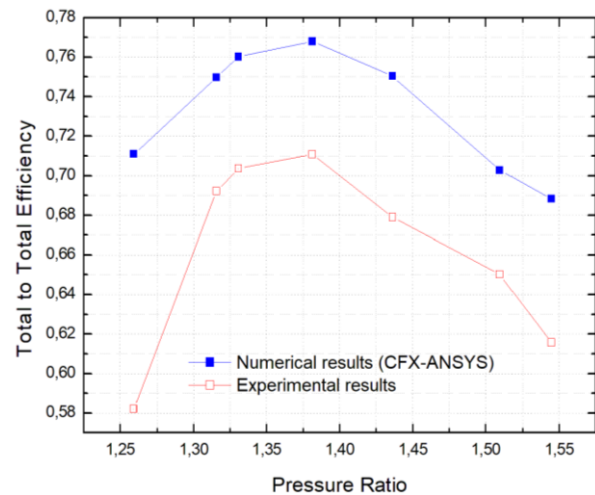
$$\dot{m}_r = 10^5 \dot{m} \sqrt{T_{0^*}}/P_{0^*} \quad (2)$$

The computational domain shown in Figure 5 does not include the spiral part (volute) of the turbine stage. As a way to evaluate the numerical and experimental results for the static efficiency with the total efficiency (eq. 3), it was essential to evaluate the volute contribution in the decrease of the turbine's overall efficiency.

$$\eta_{TS} = \frac{h_{in^*} - h_{out}}{C_p \cdot T_{in^*} \cdot [1 - (P_{out}/P_{in^*})]^{(\gamma-1)/\gamma}} \quad (3)$$

Figure 12 shows us that with a 50 % of rotational speed, the total to static efficiency has indeed reached its peak at a pressure ratio equal to 1.38. This operating point offers a compromise between the peak of efficiency and this value of pressure ratio.

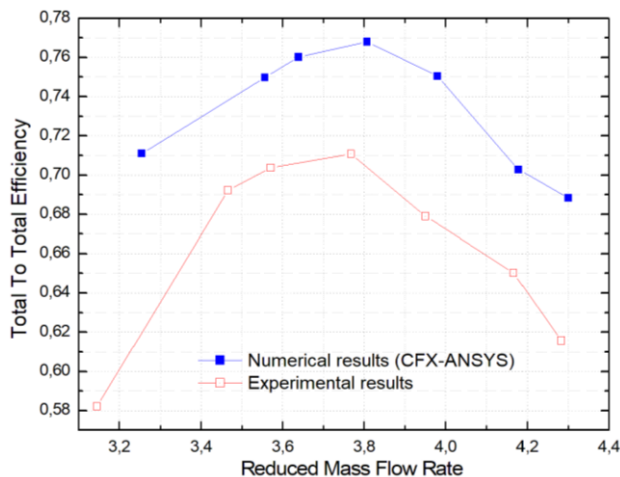
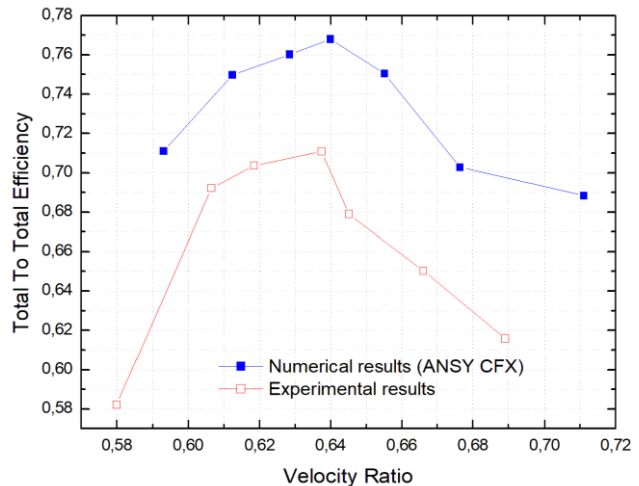
Despite the fact the suitable agreement is obtained at each rotational speed for high-pressure ratios, the turbulent flow model used in this calculation fails to be predicting the appropriate efficiency at lower ones. This defection may be attributed to the k-ε turbulence model used in this simulation. It need to be mentioned that k-ε models like other two-equation models, which are suitable for many flows of technical interest, become limited in applications with boundary layer separation and flows with sudden changes in strain rate. medium, such as those encountered in a turbomachine [17]. Figure 13 presents the variation of the total to static efficiency as a function of the reduced mass flow rate. We notice that the efficiency of the radial inflow turbine increases proportionally as a function of the pressure ratios until reaching a maximum value, beyond this value, total to static isentropic efficiency gradually decreases with increasing reduced mass flow rate.


Figure 11 Reduced mass flow rate characteristics

Figure 12 Total to static efficiency vs pressure ratio

The total to static aerodynamic efficiency measured for radial inflow turbine are plotted against the velocity ratio U/C (eq. 4) in figure 14. It is apparent that the constant blade angle design in fact maintains higher efficiencies across the full operating range than the constant incidence design. The efficiency of this turbine in particular exceeded expectation, with the peak efficiency (≈ 0.77) occurs at about $U/C = 0.64$ which is slightly higher than the target, but at lower pressure ratios this drops well below 0.6.

$$UC = \frac{U_2}{C_{0*}} \quad (4)$$

where U_2 and C_0 are respectively the peripheral speed and the expansion speed.


Figure 13 Total to static efficiency vs reduced mass flow

Figure 14 Total to static efficiency vs velocity ratio

3.4. Flow Analyses

The distribution of the static pressure and the speed vectors at different pressure ratios are presented on figures 15 to 19. The blade loading is illustrated by the static pressure contours around the pressure and suction sides of the blade. The blade geometry generates the pressure gradient between the suction and pressure sides, resulting in the torque transmitted to the blade. These figures confirm that the flow velocities on the suction side are higher than the velocities on the pressure side. Note that for this speed and for all pressure ratios, there is always a two pressure drop zones at the suction side, as predicted, this pressure drop reflect the presence of

two recirculation zones which are due to the pressure gradient. This recirculation zones for such rotational speed is almost stationary. We can notice that the two recirculation zones tends to slowly weaken when increasing the pressure ratios (Figure 19), this explains the sensitivity of the flow at low rotation speeds and low pressure ratios. From reading the figures, it can be also observed that when the fluid flows further down along the blade passage, it expands smoothly through the rotors. It reveals that there is a large pressure gradient across the rotor inlets, with higher pressure occurring at the shroud. This pressure gradient is necessary to balance the difference in centrifugal force between the shroud and hub, resulting from the change of radius. This suggests that any design procedure of radial inflow turbines with low hub-to tip-radius ratio should take into account this radial effect.

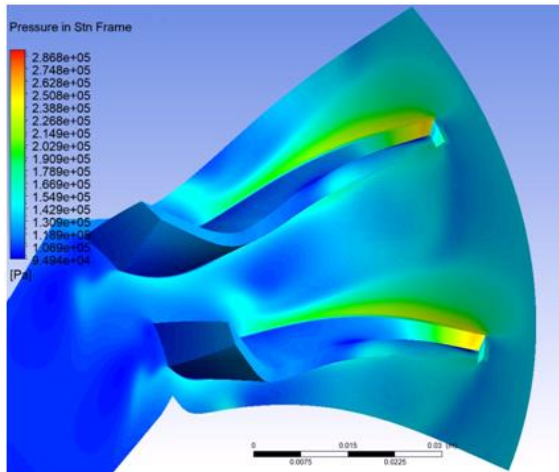


Figure 15 Pressure contours distribution in mid span of the blade to blade channel ($Pr = 1.21818$)

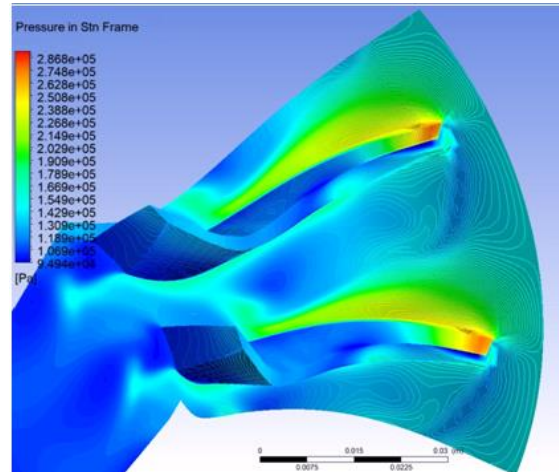


Figure 16 Pressure contours distribution in mid span of the blade to blade channel ($Pr = 1.43618$)

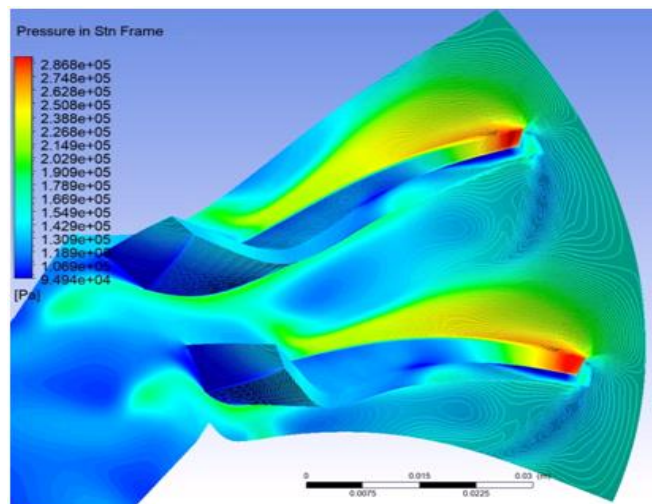


Figure 17 Pressure contours distribution in mid span of the blade to blade channel ($Pr = 1.54471$)

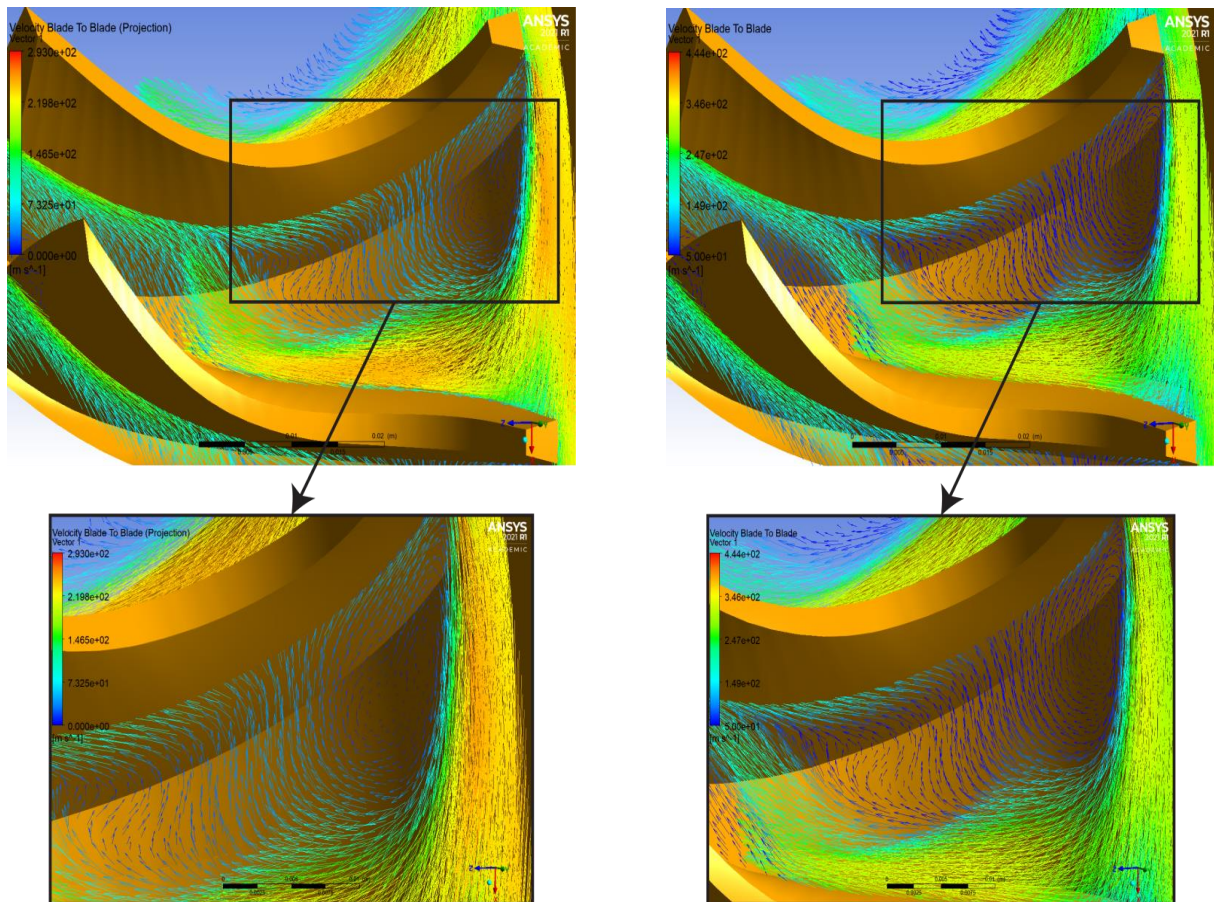


Figure 18 Velocity vectors distribution in mid span of the blade to blade channel ($Pr = 1.21818$) **Figure 19** Velocity vectors distribution in mid span of the blade to blade channel ($Pr = 1.54471$)

3.5. Influence of the Blade number on the Turbine Performances

In order to obtain better efficiency under design conditions (Table 1), the geometry of the radial flow turbine need to be optimized. Theoretical and experimental research show that the geometric characteristics and the blades number have a remarkable influence on the flow passage and the efficiency of the turbine. Five simulations are performed on rotors with different blades numbers (10, 12, 14, 16, and 18) having the identical geometric form. The outcomes proven in Figure 20 in terms of total static efficiency show that the 12-blade rotor has the very best efficiency under the design conditions. The studies performed within the literature led us to examine the most excellent number of slides with that obtained using empirical formulation. Applying the empirical formulation proposed by Jamieson, Glassman, Whitfield, and Rohlik gives respectively figures 20 to 23. The range of blades closest to the existing analysis is that proposed through Rohlik.

Figures 20 and 21 show the total pressure variation to total pressure ratio of the turbine with respect to the variation in the number of blades, this variation indicates poor expansion when a low number of blades is used, resulting in losses of high output [18]. The torque developed by all the blades is shown in figure 22, the maximum torque is produced with 12 rotor blades. The torque developed by a single blade is shown in figure 23.

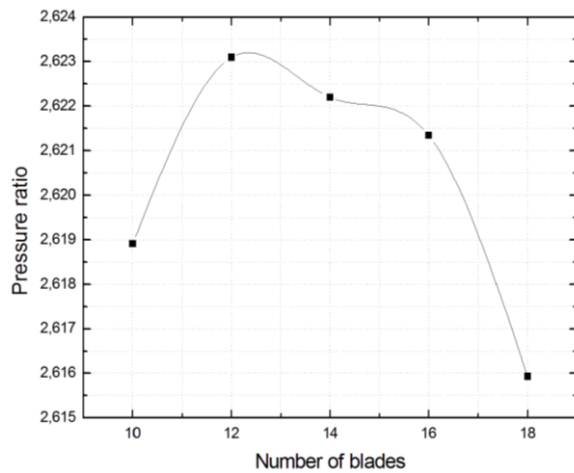


Figure 20 Pressure ratio vs number of blades

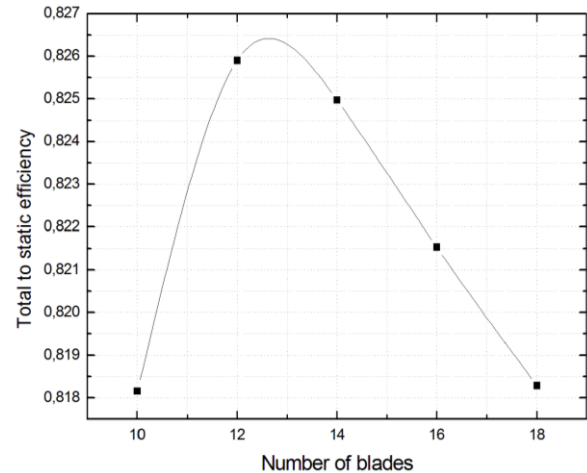


Figure 21 Total to static efficiency vs Number of blades

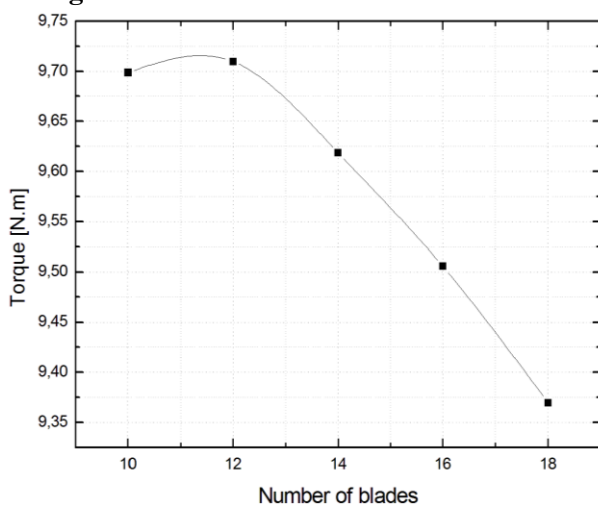


Figure 22 Torque developed by the rotor (all blades)

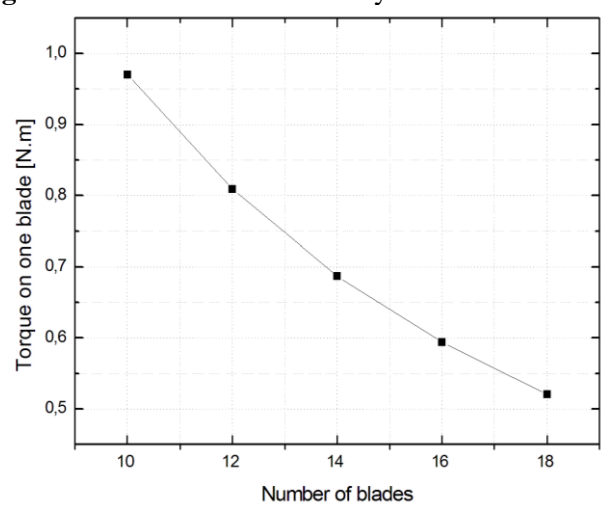


Figure 23 Torque developed by a single blade

It is found that under the design conditions, the 12-blade radial flow turbine reveals higher performance. This number of blades is recommended for this turbine. While the usage of a large number of blades, the spacing between blades is reduced, the fluid then has a tendency to be higher guided, however the losses because of friction might be more. The 12-bladed rotor gives a compromise between good guidance and minimization of losses. The pressure distribution around the blade of the five rotors is shown in figure 24, all these rotors show a positive pressure gradient on the suction aspect of the blade, which produces boundary layer separation and recirculation of the blade flux. It is able to be seen that because the number of blades will increase, the pressure difference between the two sides of the blade has the tendency to decrease, the recirculation region which represents a loss of energy disappears. The appropriate pressure distribution appears to be the twelve-bladed rotor.

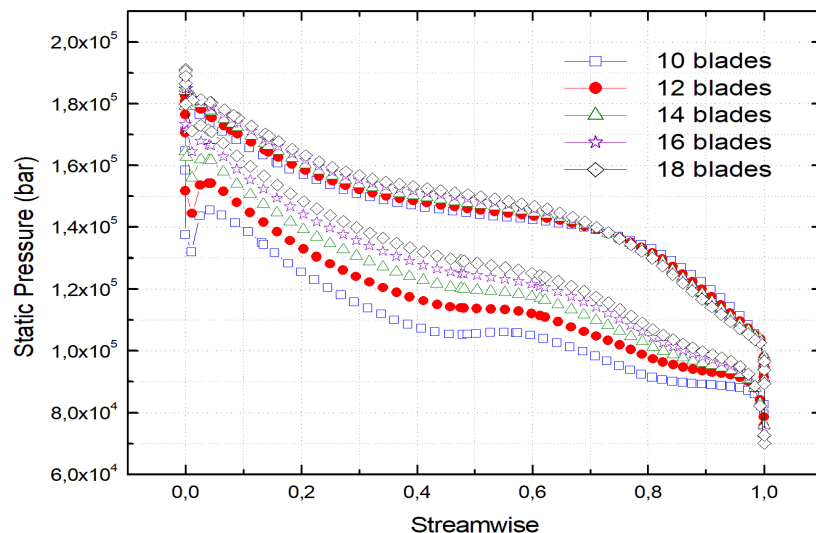


Figure 24 Normalized streamwise (0-1)

4. CONCLUSION

This paper presents a numerical prediction of the performance of a radial inflow turbine under constant inlet flow conditions. The ANSYS-CFX code is employed to solve the highly three-dimensional compressible, viscous and turbulent flow in the radial flow turbine. The numerical values of total-to-total efficiency calculated at the steady state are in reasonable agreement with the experimental data. The maximum efficiency for 50 percent of the rotational speed occurs at a speed ratio lower than the 0.70 usual for radial turbines. The optimum number of blades is always desirable to avoid flow reversals and give better flow guidance, to the detriment of increased friction losses, inertia, flow blockages, weight, and cost of the machine. To do this, numerical simulations were carried out to study a three-dimensional flow path in the rotor with a variable number of blades. It is of primary interest to focus on efficiency, power, the torque developed, and the pressure ratio of the results. All the curves are of similar shape and have an optimum value corresponding to the number of blades equal to 12. This could be due to a better distribution of the load on the blades, with a minimum flow reversal effect and better guidance of the flow. Outside of this optimal value, the trends are reversed. The magnitude of all performance variables decreases, certainly due to inertia, frictional losses, and the blocking effect. It could conclude from previous discussions that the peak performance and efficiency of the turbine is a compromise between a blades defined number.

REFERENCES

- [1] C. Rodgers, R. Geiser, Performance of a High-Efficiency Radial/Axial Turbine, Journal of Turbomachinery, ASME, vol. 109 no 2, pp. 151-154, Apr 1987, <https://doi.org/10.1115/1.4049776>
- [2] S. L. Dixon, Fluid mechanics, thermodynamics of turbomachinery, Fourth edition in SI/METRIC UNITS, Oxford, 1998.
- [3] H. E. Rohlik, Analytical determination of radial-inflow turbine design geometry for maximum efficiency, NASA TN D-4384, USA, February 1968.
- [4] C. Todd, S. M. Jr. Futral, A Fortran IV program to estimate the off-design performance of radial inflow turbines, NASA TN D-5059, USA, March 1969.

- [5] S. M. Jr. Futral, C.A. Wasserbauer, Off-design performance prediction with Experimental Verification for a Radial Inflow Turbine, NASA TN D-2621, USA, 1965, <https://searchworks.stanford.edu/view/8599447>
- [6] C. A. Wasserbauer, A. J. Glassman, Fortran program for predicting off-design performance of radial inflow turbines, NASA TN D-8063, USA, 1975.
- [7] L. Angelo, Radial turbine preliminary design and performance prediction, AIP Conference Proceedings, vol. 2191 no 1, 020097, Italy, December 2019, <https://doi.org/10.1063/1.5138830>
- [8] U. Khairuddin, A. W. Costall, R. F. Martinez-Botas, Influence of Geometrical Parameters on Aerodynamic Optimization of a Mixed-Flow Turbocharger Turbine, Turbine Technical Conference and Exposition, ASME, Turbo Expo, GT2015-42053, Vol. 2C, June 15-16, Montreal-Canada, 2015, <https://doi.org/10.1115/GT2015-42053>
- [9] J. Zhang, M. Zangeneh, A 3D inverse design based multidisciplinary optimization on the radial and mixed-inflow turbines for turbochargers, 11th International Conference on Turbochargers and Turbocharging, pp. 399-410, May 13-14, London, 2014, <http://doi.org/10.1533/978081000342.399>
- [10] L. M. Kerry, E. H. Jeffry, Experimental performance and analysis of Radial-Inflow turbine with work factor of 1.126 and tick blading, NASA Technical Paper 1730, USA, 1980, <https://ntrs.nasa.gov/citations/19800024902>
- [11] H. Chen, M. Abidat, N. C. Baines, M. R. Firth, The effect of Blade Loading in Radial and Mixed Flow Turbines, International Gas Turbine and Aeroengine Congress and Exposition, 92-GT-092, V001T01A049, Cologne-Germany, June 1992, <https://doi.org/10.1115/92-GT-092>
- [12] S. V. Patankar, D. B. A. Spalding, Calculation procedure for heat, mass and momentum transfer in three-dimensional parabolic flows, International journal of heat and mass transfer, vol. 15 no 10, pp. 1778-1806, 1972, http://ftp.demec.ufpr.br/CFD/bibliografia/Patankar_Spalding_1972.pdf
- [13] ANSYS CFX, Solver Theory guide, Academic Research Release 11, ANSYS Inc, 2006.
- [14] C. M. Rhie, W. L. A. Chow, Numerical Study of the Turbulent Flow Past an Airfoil with Trailing Edge Separation, AIAA journal, vol 21 no 11, pp. 1525-1532, November 1983, <https://arc.aiaa.org/doi/pdf/10.2514/3.8284>
- [15] K. R. Pullen, The design and development of a small gas turbine and high speed generator, Doctoral dissertation, Imperial College, London, 1991.
- [16] I. B. Celik, U. Ghia, P. J. Roache, Procedure for estimation and reporting of uncertainty due to discretization in CFD applications, Journal of fluids (Engineering-Transactions), ASME, vol. 130 no 7, 078001, July 2008, <https://doi.org/10.1115/1.2960953>
- [17] M. Abidat, M. K. Hamidou, M. Hachemi, M. Hamel, S. A. Litim, Performance prediction of a Mixed Flow Turbine, Mécanique & Industries, vol. 9 no 1, pp. 71-79, January 2008, <https://doi.org/10.1051/meca:2008009>
- [18] A. Ketata, Z. Driss, Abid, Impact of blade number on performance, loss and flow characteristics of one mixed flow turbine, Energy, vol. 203, 117914, July 2020, <https://doi.org/10.1016/j.energy.2020.117914>